

# Simulation Results for Permutation Trellis Codes using M-ary FSK

T.G. Swart, I. de Beer, H.C. Ferreira

Department of Electrical and Electronic Engineering  
University of Johannesburg  
Auckland Park, South Africa  
{ts,idb,hcf}@ing.rau.ac.za

A.J.H. Vinck

Institute for Experimental Mathematics  
University of Essen  
Essen, Germany  
vinck@exp-math.uni-essen.de

**Abstract**—It has previously been shown that using the combination of permutation codes and M-ary frequency shift keying has special properties and error correcting capabilities that are suitable for the noise types encountered in power line communications. Furthermore, the permutation codes are used to map onto the outputs of a binary convolutional code to form permutation trellis codes. We investigate and compare the performance of different permutation trellis codes when used with M-FSK for power line communications.

**Keywords**—channel coding; convolutional codes; interference suppression

## I. INTRODUCTION

Previous research [1,2] has shown how combining M-ary frequency shift keying (M-FSK) with permutation codes can be used to correct broad-, narrowband and background noise. A quick overview of this is given in Section II. It has also been shown [3] how distance mappings can be used to map permutation codes onto the outputs of a binary convolutional code to form permutation trellis codes. This is covered in a brief overview in Section III. Section IV discusses the simulations and the results obtained for various mappings of permutation trellis codes.

## II. PERMUTATION CODES AND M-ARY FSK

The definition for a permutation code is as follows:

*Definition 1:* A permutation code  $C$  consists of  $|C|$  code words of length  $M$ , where every code word contains the  $M$  different integers  $1, 2, \dots, M$  as symbols.

Every symbol corresponds uniquely to a frequency from an M-FSK modulator. The M-ary symbols are transmitted in time as the corresponding frequencies, thus the transmitted signal has a constant envelope.

The demodulator consists of a modified envelope detector for each frequency, that outputs a 1 if the signal envelope is above a certain threshold and outputs a 0 otherwise. Thus for each symbol transmitted,  $M$  outputs are obtained from the demodulator. These result in an  $M \times M$  binary matrix that is used for decoding, where the rows represent the frequencies used and the columns represent the position or time in the code word. When combined with convolutional codes (as described

in the next section) this binary matrix is used in the Viterbi decoder.

*Example 1:* The  $M=4$  permutation code word (1,4,2,3) is sent. If received correctly, the output of the demodulator would be

$$\begin{array}{cccc}
 f_1 & 1 & 0 & 0 & 0 \\
 f_2 & 0 & 0 & 1 & 0 \\
 f_3 & 0 & 0 & 0 & 1 \\
 f_4 & 0 & 1 & 0 & 0 \\
 & t_1 & t_2 & t_3 & t_4
 \end{array}$$

where  $f_i$  represents the output for the detector at frequency  $i$  and  $t_j$  represents the time interval  $j$  in which it occurs, for  $1 \leq i, j \leq 4$ .

Channel noise causes errors in the matrix, which can be represented by the following:

- background noise – insertion or deletion of ones

$$\begin{array}{cccc}
 \underline{0} & 0 & 0 & 0 \\
 0 & 0 & 1 & 0 \\
 0 & \underline{1} & 0 & 1 \\
 0 & 1 & 0 & 0
 \end{array}$$

- impulse noise – a complete column is set to ones

$$\begin{array}{cccc}
 1 & 0 & \underline{1} & 0 \\
 0 & 0 & \underline{1} & 0 \\
 0 & 0 & \underline{1} & 1 \\
 0 & 1 & \underline{1} & 0
 \end{array}$$

- narrowband noise – a complete row is set to ones

$$\begin{array}{cccc}
 1 & 0 & 0 & 0 \\
 0 & 0 & 1 & 0 \\
 0 & 0 & 0 & 1 \\
 \underline{1} & \underline{1} & \underline{1} & \underline{1}
 \end{array}$$

### III. PERMUTATION TRELLIS CODES

Using convolutional codes it is possible to easily decode permutation codes using a trellis and the Viterbi algorithm. The outputs of a binary convolutional encoder are mapped onto the code words from a permutation code. A mapping consists of choosing an ordered subset of  $2^n$   $M$ -tuples, from the full set of permutation  $M$ -tuples, to map onto the corresponding convolutional base code's  $n$ -tuples. The subset is chosen such that the Hamming distance between any two permutation  $M$ -tuples is at least as large as the distance between the corresponding convolutional code's output  $n$ -tuples which are mapped onto them. This property was previously called distance preserving in [4], since the Hamming distance of the base code is at least conserved, and may sometimes even be increased in the resulting trellis code.

*Example 2:* Using the standard  $R=1/2$ ,  $v=2$ ,  $d_{\text{free}}=5$  convolutional code, we map  $n=2 \rightarrow M=3$  by applying the following mapping:  $\{00,01,10,11\} \rightarrow \{231,213,132,123\}$ . This results in the state systems as shown in Fig. 1.

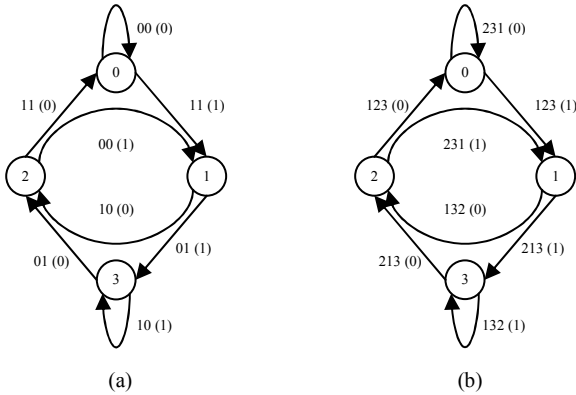


Figure 1. State systems for (a) convolutional base code and (b) permutation trellis code

It can easily be verified that the distance between any permutation code words and the corresponding binary outputs increases by one. The shortest remerging paths in the trellis, which for this code determines the free distance, have a length of three steps. Thus for each step there is an increase in distance of one, resulting in a free distance of  $d'_{\text{free}}=8$  for the permutation trellis code.

Three different mappings can be obtained, depending on how the Hamming distance is preserved:

- distance conservative mapping (DCM) – guarantees conservation of the base code's free distance
- distance increasing mapping (DIM) – guarantees that the resulting trellis code's distance will always have some increase above the base code's free distance
- distance reducing mapping (DRM) – has a distance loss which is guaranteed to be not more than a fixed amount per step between any two unremerged paths in the trellis diagram of the resulting trellis code.

### IV. SIMULATION RESULTS

A simple error model, which generates errors in the received matrix according to certain error parameters, was used to evaluate the different mappings. The error parameters were assumed to be equal for all frequency sub-bands. The different types of noise are generated as follows (similar to Example 1):

- background noise – each element in the received matrix has a probability,  $p_b$ , of being in error
- impulse noise – each column in the received matrix has a probability,  $p_i$ , of resulting in an impulse noise
- permanent frequency disturbance (or narrowband noise) – all received matrices will have 1's in the row that corresponds to the frequency error

The following mappings were used: (1) DIM, mapping  $n=4$  onto  $M=5$  while increasing the distance by 1, found by trail and error, (2) DCM<sub>1</sub>, mapping  $n=5$  onto  $M=5$  while conserving the distance, obtained by applying the prefix construction method from [3], (3) DCM<sub>2</sub>, mapping  $n=5$  onto  $M=5$  while conserving the distance, found by exhaustive search, and (4) DRM, mapping  $n=6$  onto  $M=5$  while decreasing the distance by at most 1, found by trail and error. The exact mappings used can be found in Table I.

TABLE I. DISTANCE MAPPINGS USED TO OBTAIN RESULTS

Description	Mapping <sup>a</sup>
$n=4 \rightarrow M=5$ DIM	$\left\{ \begin{array}{l} 12345, 13452, 14523, 15234, 23514, 25143, \\ 21435, 24351, 31542, 32154, 34215, 35421, \\ 52413, 53241, 51324, 54132 \end{array} \right\}$
$n=5 \rightarrow M=5$ DCM <sub>1</sub>	$\left\{ \begin{array}{l} 51234, 51243, 51324, 51342, 51423, 51432, \\ 52134, 52143, 53214, 53241, 52314, 52341, \\ 53421, 53412, 53124, 53142, 41235, 41253, \\ 41325, 41352, 41523, 41532, 42135, 42153, \\ 43215, 43251, 42315, 42351, 43521, 43512, \\ 43125, 43152 \end{array} \right\}$
$n=5 \rightarrow M=5$ DCM <sub>2</sub>	$\left\{ \begin{array}{l} 12534, 21435, 13254, 24153, 21354, 12345, \\ 23514, 23145, 15243, 51423, 25134, 53241, \\ 41325, 21543, 31524, 35142, 14235, 12453, \\ 34251, 54132, 42513, 32415, 34512, 43152, \\ 54321, 52431, 45231, 35421, 52314, 45312, \\ 43521, 53412 \end{array} \right\}$
$n=6 \rightarrow M=5$ DRM	$\left\{ \begin{array}{l} 12345, 12354, 12543, 12534, 13245, 13254, \\ 13542, 13524, 14325, 14352, 14523, 14532, \\ 15324, 15342, 15423, 15432, 21345, 21354, \\ 21543, 21534, 23145, 23154, 23541, 23514, \\ 24315, 24351, 24513, 24531, 25314, 25341, \\ 25413, 25431, 42153, 42135, 42513, 42531, \\ 41253, 41235, 41523, 41532, 45123, 45132, \\ 45213, 45231, 43251, 43215, 43521, 43512, \\ 32154, 32145, 32514, 32541, 31254, 31245, \\ 31524, 31542, 35241, 35214, 35421, 35412, \\ 34251, 34215, 34521, 34512 \end{array} \right\}$

a. Binary code words have been omitted. Use normal lexicographical ordering.

These  $M=5$  mappings were used as follows: (1) DIM was mapped onto a rate  $R=3/4$ ,  $v=2$ ,  $d_{\text{free}}=3$ , punctured convolutional base code, (2)  $\text{DCM}_1$  and (3)  $\text{DCM}_2$  were mapped onto a rate  $R=3/5$ ,  $v=2$ ,  $d_{\text{free}}=4$ , punctured convolutional base code, and (4) DRM was mapped onto a rate  $R=3/6$ ,  $v=2$ ,  $d_{\text{free}}=5$ , punctured convolutional base code. These rates ensured that the overall system rate was the same in all four cases. Also, in all cases the guaranteed free distance of the permutation trellis code,  $d_{\text{free}}$ , is equal to 4.

The mappings only guarantee a minimum increase or maximum loss of distance. Thus it is generally able to exceed these, with even the DRM showing an increase of distance on average. For the mappings used, we have an average distance increase as follows: (1) DIM with 2.10, (2)  $\text{DCM}_1$  with 1.06, (3)  $\text{DCM}_2$  with 1.54, and (4) DRM with 0.91. This would suggest that the  $\text{DCM}_2$  should perform better than the  $\text{DCM}_1$ .

Fig. 2 compares the mappings when only one permanent frequency disturbance occurs in the presence of background noise. This was done with the disturbance present on a different frequency position each time. The DIM is performing the best, with the performance irrespective of which frequency the disturbance is on. The  $\text{DCM}_1$  is the worst with performance varying, depending on the position of the disturbance.

Fig. 3 compares the mappings when zero, one (in position 1), two (in positions 1 and 2) and three (in positions 1, 2 and 3) frequency disturbances respectively occur at the same time in the presence of background noise. Again, the DIM is performing the best, with the  $\text{DCM}_2$  and DRM very close to each other. While the  $\text{DCM}_1$  was close to the others for no disturbances, its performance degrades significantly as the number of disturbances increases. The previous result has

shown that this mapping's performance depends on the disturbance positions, thus certain combinations of disturbances can render it useless (as in the case of three disturbances on positions 1, 2 and 3). Other combinations might result in slightly better performance.

## V. CONCLUSION

Various simulation results have been presented for different mappings to be used with permutation trellis codes combined with M-FSK. The effect of permanent frequency disturbances in the presence of background noise was investigated, taking into account the position and number of disturbances. The results gave a clear indication of how the various mappings performed under these conditions.

## REFERENCES

- [1] A.J.H. Vinck, "Coded Modulation for Powerline Communications," *AEU International Journal of Electronics and Communications*, vol. 54, no. 1, pp. 45-49, 2000.
- [2] A.J.H. Vinck, A. Hasbi, H.C. Ferreira and T.G. Swart, "On Coded M-ary Frequency Shift Keying," *Proceedings of the International Symposium on Power Line Communications 2004*, Zaragoza, Spain, pp. 175-179, March 31-April 2, 2004.
- [3] H.C. Ferreira and A.J.H. Vinck, "Interference Cancellation with Permutation Trellis Codes," *Proceedings of the IEEE Vehicular Technology Conference Fall 2000*, Boston, MA., U.S.A., pp. 2401-2407, September 24-28, 2000.
- [4] H.C. Ferreira, D.A. Wright and A. L. Nel, "Hamming Distance Preserving Mappings and Trellis Codes with Constrained Binary Symbols," *IEEE Transactions on Information Theory*, vol. 35, no. 5, pp. 1098-1103, September 1989.

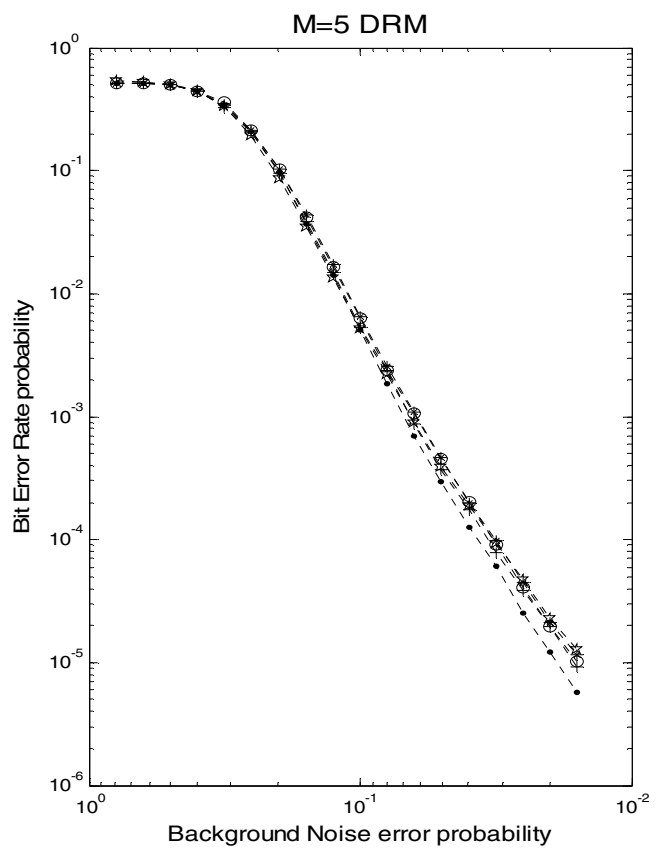
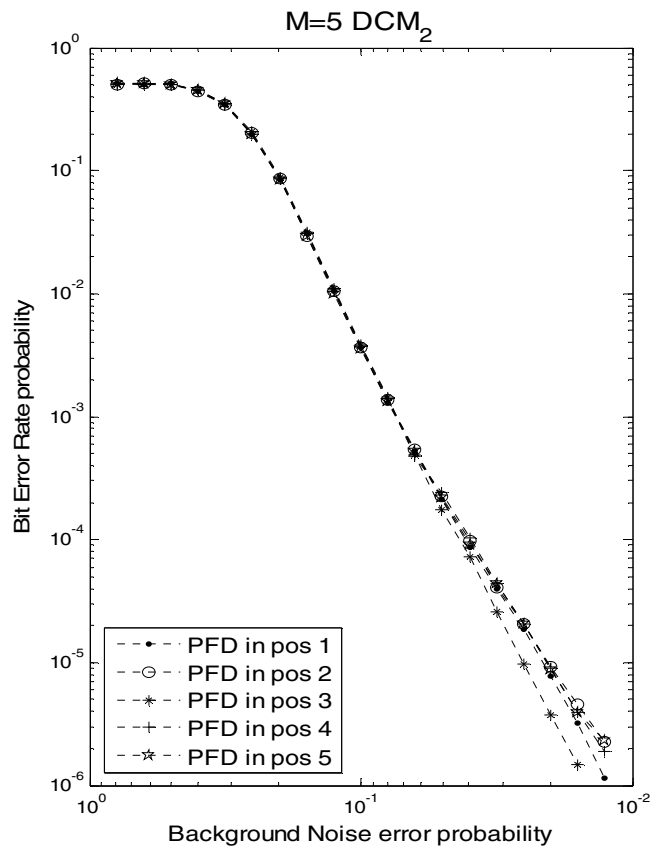
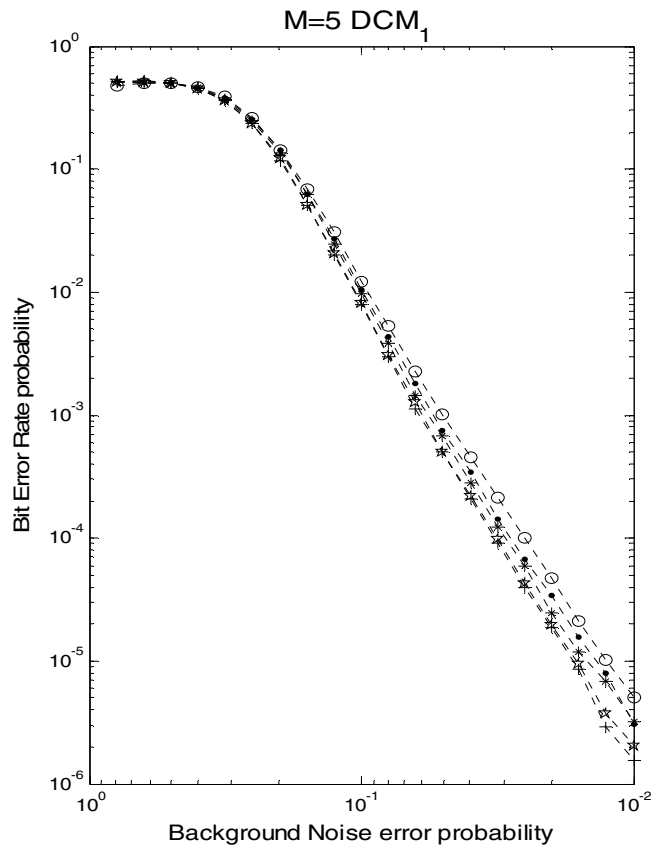
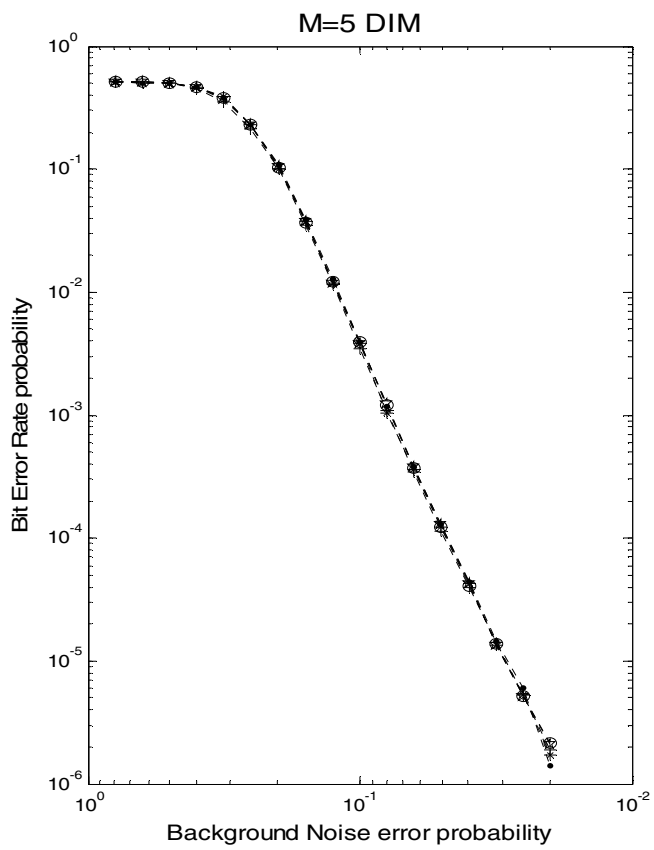


Figure 2. Single permanent frequency disturbance (PDF) in different positions

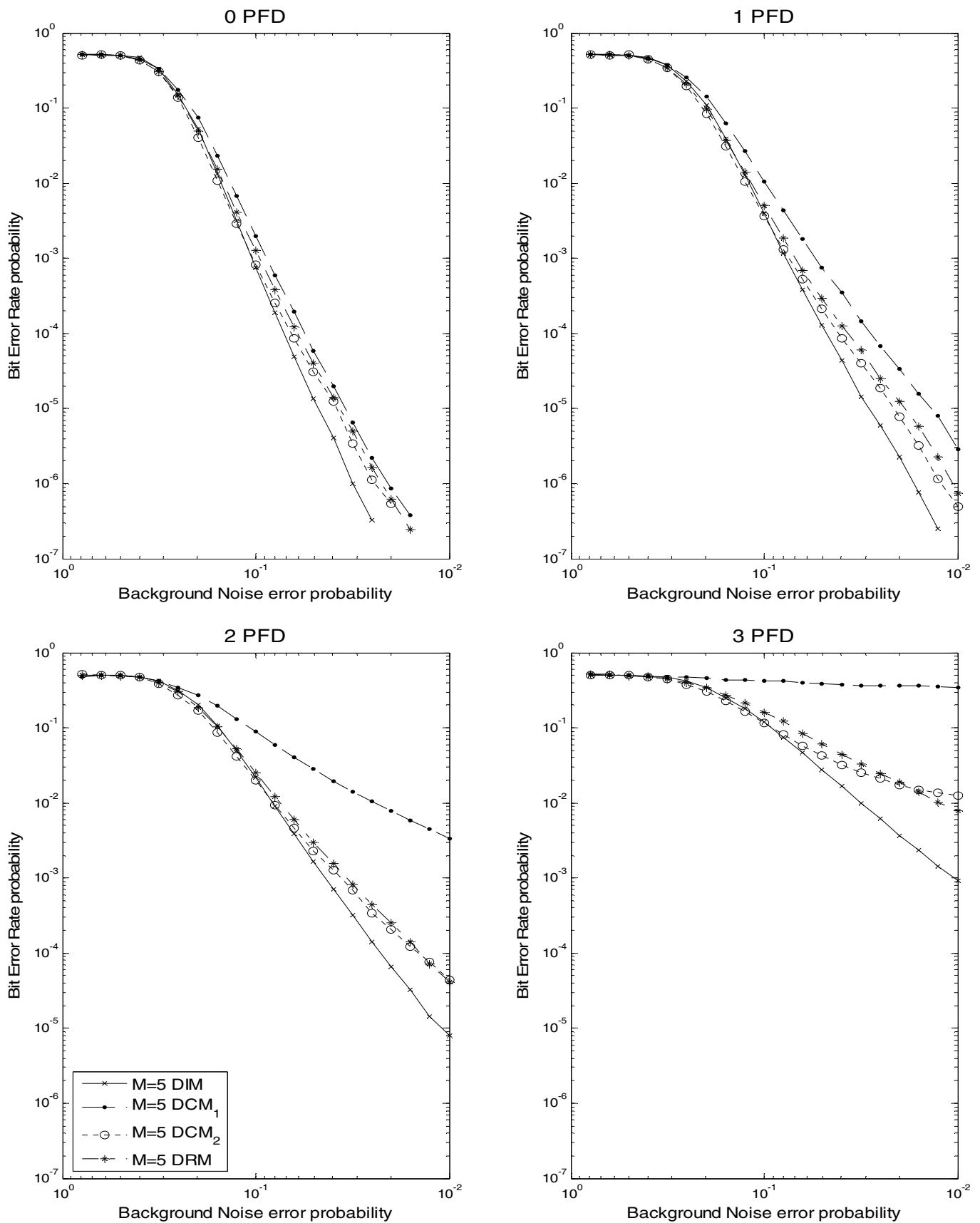


Figure 3. Comparison of various number of permanent frequency disturbances (PFD)